Posted: May 28, 2026

Event-Specific Time of Concentration and Hydrological Signature from IBER Hydrographs: A Proof-of-Concept Framework with Uncertainty Quantification

Integrating GLUE, Bootstrap BCa, synthetic unit hydrographs, and flow-duration curve analysis

Mauricio Javier Victoria Niño[1]

[1]Independent researcher, Cali, Colombia; hidratecsa@gmail.com; ORCID: 0009-0003-4328-5691

This document is a preprint that has not been peer-reviewed, submitted to EngrXiv. Source code and example data are available at: https://github.com/MauricioVictoriaN/IBER_TcEstimator.

Abstract

Context and motivation. Conventional hydrological practice treats the Time of Concentration (T_c) as an intrinsic, invariant watershed property estimated through empirical formulas. This assumption introduces significant uncertainty when T_c is used in semi-distributed models for extreme-event design, particularly in large watersheds where storage, attenuation and nonlinear flow effects dominate the hydrograph shape.

Objective. This paper presents IBER_TcEstimator v1.0, an open-source R framework that extracts event-specific T_c estimates—with formal uncertainty quantification—from IBER hydrographs, and characterises the event through a hydrological signature analysis.

Methods. The framework integrates five modules: (A) uncertainty quantification via GLUE and Bootstrap BCa; (B) baseflow separation with three recursive digital filters; (C) effective precipitation via CN-NRCS; (D) generation of SCS, Clark and GIUH synthetic unit hydrographs plus Tikhonov deconvolution; and (E) advanced diagnostics including KGE, NSE, PBIAS, Durbin-Watson and Ljung-Box tests, $T_c \to Q_p$ elasticity, and hydrological event signature (FDC, Richards-Baker flashiness index, recession slope).

Proof-of-concept results. On a synthetic $150.5\,\mathrm{km}^2$ watershed (CN = 82, $L_c = 28.36\,\mathrm{km}$, $S = 0.0073$), the SCS Lag method yields $T_c = 17.85\,\mathrm{h}$—2.1 to 7.1 times larger than six empirical formulas (Kirpich: $2.5\,\mathrm{h}$; Temez: $7.96\,\mathrm{h}$)—with a 95 % BCa Bootstrap CI of [13.02, 22.59] h (convergence verified: 0.76 % relative CI width difference). GLUE produces a posterior median of $16.20\,\mathrm{h}$ (95 % CI: [12.71, 19.75] h) with 31.6 % behavioural realisations (KGE $\geq$ 0.50). Performance metrics indicate good-to-very-good shape fit (KGE = 0.667, NSE = 0.808), with a volumetric bias (PBIAS = 26.64 %) and strong residual autocorrelation (DW $\approx$ 0, LB = 27 553, $p < 0.001$) explicitly characterised. The event FDC reveals a highly attenuated response (R-B flashiness index = 0.0009) with very slow recession (slope = 0.0179 decades per percentage point). Three baseflow filters yield a narrow BFI range of 0.82–0.85 (CV < 2 %). The record duration ($14\,\mathrm{h}$) is 0.78 times T_c, below the recommended ratio of 2.5 for reliable baseflow separation.

Limitations and outlook. As a *proof-of-concept*, results are based on a synthetic watershed. Validation

against real gauged catchments, multi-event analysis, and global sensitivity analysis are the primary next steps.

Keywords: Time of concentration; IBER; synthetic unit hydrograph; GLUE; baseflow separation; hydrological event signature; CN-NRCS; hydrological uncertainty; Nash-Sutcliffe efficiency; Durbin-Watson test; Shapiro-Wilk test; proof-of-concept; R software.
Software availability: IBER_TcEstimator v1.0 is open-source at https://github.com/MauricioVictoriaN/IBER_TcEstimator (MIT licence).

List of Acronyms

Acronym	Full form
BCa	Bias-corrected and accelerated (Bootstrap)
BFI	Baseflow Index
CI	Confidence interval
CN	Curve Number (NRCS method)
CV	Coefficient of variation
DW	Durbin-Watson (test statistic)
FDC	Flow Duration Curve
GIUH	Geomorphoclimatic Instantaneous Unit Hydrograph
GLUE	Generalised Likelihood Uncertainty Estimation
HU	Unit Hydrograph
IBER	2D finite-volume hydraulic-hydrological model
ISO	International Organization for Standardization
KGE	Kling-Gupta Efficiency
KGE″	Modified Kling-Gupta Efficiency (Kling et al., 2012)
LB	Ljung-Box (test statistic)
LOESS	Locally Estimated Scatterplot Smoothing
NRCS	Natural Resources Conservation Service (USDA)
NSE	Nash-Sutcliffe Efficiency
PBIAS	Percent Bias
PBPF	Peak Bias in Peak Flow
R-B	Richards-Baker (flashiness index)
RMSE	Root Mean Square Error
SCS	Soil Conservation Service (former name of NRCS)
SUH	Synthetic Unit Hydrograph
T_{50}	Time to centroid (50 %) of effective precipitation
UH	Unit Hydrograph
WMO	World Meteorological Organization

1 Introduction

The Time of Concentration (T_c) is one of the most widely used parameters in hydrological design: it defines the critical storm duration for peak-discharge computation, governs the shape of the design hydrograph, and is directly embedded in the unit-hydrograph theory underlying tools such as HEC-HMS [7, 53]. Despite its central role, T_c estimation remains one of the most uncertain steps in the hydrological design chain, with published formulas often producing estimates that differ by an order of magnitude for the same watershed [21, 16].

Conventional practice estimates T_c from empirical formulas calibrated on specific geomorphological and climatic contexts—Kirpich [27], Temez [49], Bransby-Williams [6], SCS Lag [40]—calibrated on datasets that often lacked information on the interrelationships between watershed characteristics [19]. The result is treated as a static, event-independent property. Several studies have challenged this assumption: T_c varies with rainfall intensity, antecedent soil moisture, and event magnitude [54, 15, 34]. McCuen et al. [33] showed that empirical formulas designed for small agricultural watersheds can produce severe errors when applied to large or complex basins. Gericke and Smithers [16] reviewed 26 methods and found inter-method variability of up to 500 % on ungauged catchments.

The IBER model [4]—a two-dimensional, finite-volume hydraulic solver widely used in Spain and Latin America for flood inundation and design-storm analysis—produces high-resolution runoff hydrographs that implicitly encode the full physics of flow routing, attenuation and storage for a given design event. Since version 3, IBER incorporates a fully distributed hydrological module [5] that resolves the rainfall-runoff transformation over the entire catchment using the 2D shallow-water equations, coupled with spatially distributed infiltration (Green-Ampt or CN-NRCS), subsurface flow, evapotranspiration, and percolation processes. This distributed module operates on the same finite-volume mesh as the hydrodynamic engine, making the simulated outlet hydrograph a direct, physically consistent product of the rainfall input, terrain topography, and soil properties. Yet no standardised, open-source protocol exists for extracting event-specific T_c from IBER outputs in a reproducible, uncertainty-aware manner. Practitioners currently rely on empirical formulas applied independently of the IBER simulation, discarding the dynamic information contained in the simulated hydrograph.

This paper addresses that gap by presenting IBER_TcEstimator v1.0, a modular R framework that (i) extracts T_c from IBER hydrographs via the SCS Lag method, (ii) quantifies estimation uncertainty through both Bootstrap BCa and GLUE approaches, (iii) compares multiple baseflow separation filters and synthetic unit hydrographs, and (iv) diagnoses model performance through a comprehensive set of international metrics and event signatures.

Scope declaration. This work is explicitly presented as a *proof-of-concept* demonstration. The evaluation is performed on a synthetic watershed with design-storm inputs, not on a real gauged catchment with observed discharge records. This methodological choice is intentional at this stage of development: it allows controlled, reproducible demonstration of the framework's full computational pipeline without the confounding effects of real-data uncertainty (sensor errors, rating-curve uncertainty, land-use change). The limitations of this approach and the validation roadmap are discussed explicitly in Section 7.

1.1 Research objectives

1. Estimate event-specific T_c from IBER hydrographs via SCS Lag with Bootstrap BCa and GLUE uncertainty quantification.
2. Compare three baseflow separation filters with automatic recession parameter estimation.

3. Generate and compare SCS, Clark, GIUH synthetic unit hydrographs and an empirical UH via Tikhonov deconvolution.
4. Evaluate model performance through KGE, NSE, PBIAS, peak metrics, Durbin-Watson and Ljung-Box residual diagnostics.
5. Characterise the hydrological event signature via FDC, Richards-Baker flashiness index, and recession slope.
6. Compare IBER-derived T_c against six empirical formulas and analyse the influence of record duration on estimation reliability.

2 Theoretical Background

2.1 Time of Concentration: SCS Lag method

The SCS Lag method [40] defines T_c from the hydraulic lag time:

$$\mathrm{Lag} = T_p - T_{50} \tag{1}$$

$$T_c = \frac{\mathrm{Lag}}{0.6} \tag{2}$$

The coefficient 0.6 is the empirical Lag-to-T_c ratio established by NRCS for rural catchments without significant retention [40]. It is important to note that this coefficient was calibrated on small agricultural watersheds in the eastern United States; its applicability to large Mediterranean or tropical basins should be regarded as an approximation, and constitutes one of the explicit limitations of this proof-of-concept (see Section 7).

2.2 Uncertainty quantification

2.2.1 Bootstrap BCa confidence intervals

The T_c confidence interval is computed via bias-corrected and accelerated Bootstrap (BCa, [14]) with $R = 2000$ resamples of the interpolated time series indices. The BCa method corrects for both bias and skewness in the bootstrap distribution, providing more accurate coverage than the standard percentile bootstrap. Convergence of the BCa interval with respect to R was verified by comparing results at $R = 1000$ and $R = 2000$; the relative difference in CI width was 0.76 %, confirming convergence.

The bootstrap statistic is the Lag computed on the resampled series. When a resample produces a non-finite or zero Lag (rare event due to extreme resampling), the nominal Lag is substituted as a conservative fall-back; the fraction of such substitutions is logged and reported as a diagnostic.

2.2.2 GLUE

GLUE [3] samples $N = 5000$ realisations of the T_c parameter space over $[0.05,\ 24]$ h via uniform prior distribution. For each $T_{c,i}$, the SCS unit hydrograph is convolved with the effective precipitation and the KGE likelihood measure [22] is evaluated. Behavioural realisations are those with KGE $\geq$ 0.50, a threshold consistent with the lower bound of the "satisfactory" classification of [35].

Threshold sensitivity. To assess robustness, GLUE was also run with thresholds of 0.40 and 0.60. The number of behavioural realisations changes substantially (from 24.1 % at KGE $\geq$ 0.60 to 40.8 % at KGE $\geq$ 0.40), but the posterior median T_c shifts by less than 1 h in either direction, confirming that

the central estimate is not highly sensitive to the threshold choice. This analysis is consistent with the equifinality concept in hydrological modelling [3]: multiple parameter combinations produce acceptable simulations, and the posterior distribution width—rather than a single point estimate—is the primary output of interest.

2.3 Baseflow separation

Three recursive digital filters (Table 1) share the recession constant α, estimated automatically via log-linear regression over recession segments [48]. The implementation follows ISO 748:2007 [25].

Table 1: Baseflow separation filters.

Filter	Equation	Parameters	Reference
Eckhardt (2005)	$Q_b(i) = \dfrac{(1-\mathrm{BFI})\,\alpha\,Q_b(i{-}1) + (1{-}\alpha)\,\mathrm{BFI}\cdot Q(i)}{1-\mathrm{BFI}\cdot\alpha}$	α, $\mathrm{BFI}_{\max}$	Eckhardt [13]
Chapman (1999)	$Q_b(i) = \dfrac{3\alpha-1}{3-\alpha}Q_b(i{-}1) + \dfrac{1-\alpha}{3-\alpha}\big[Q(i){+}Q(i{-}1)\big]$	α	Chapman [9]
Lyne–Hollick (1979)	$Q_d(i) = \alpha\,Q_d(i{-}1) + \dfrac{1+\alpha}{2}\big[Q(i) - Q(i{-}1)\big]$	α	Lyne & Hollick [32]

2.4 Effective precipitation: CN-NRCS method

Precipitation abstraction follows the NRCS Curve Number method [40, 39]:

$$Q_e(t) = \frac{\big[P(t) - I_a\big]^2}{P(t) - I_a + S}; \quad S = 25.4\left(\frac{1000}{\mathrm{CN}} - 10\right); \quad I_a = \lambda S,\ \lambda = 0.20 \tag{3}$$

It is noted that Hawkins et al. [24] documents an ongoing debate on the appropriate value of λ, with $\lambda = 0.05$ producing better fits in many observed datasets. For this proof-of-concept, the NRCS default $\lambda = 0.20$ is retained. Effective precipitation at each time step is obtained by differentiation: $P_e(t) = \max(0,\, Q_e(t) - Q_e(t - \Delta t))$.

2.5 Synthetic unit hydrographs

Four methods are implemented (Table 2): SCS/NRCS [40], Clark [8, 37], GIUH [42, 47], and Tikhonov deconvolution [50].

The GIUH [42] models catchment response as a gamma density function whose parameters k and m are derived from mean flow velocity v, main channel length L_c, and the Horton–Strahler bifurcation ratio R_b and length ratio R_l:

$$k = 0.44\,t_r\,(R_b/R_l)^{0.55}; \quad m = 3.29\,(R_b/R_l)^{0.78}(L_m/\sqrt{A})^{0.07} \tag{4}$$

where $t_r = L_c/v$ is the main-channel travel time and L_m is the channel length in metres. The gamma response is then convolved with effective precipitation to obtain the GIUH-based direct runoff hydrograph.

Table 2: Unit hydrograph methods.

Method	Description	Parameters	Reference
SCS/NRCS	Triangular: $T_p = D/2 + 0.6T_c$; $T_b = 2.67T_p$; $q_p = 0.208A/T_p$	T_c, D, A	NRCS [40]
Clark	Elliptic time-area + linear reservoir; storage coefficient R approximated as $R = T_c$ when not independently calibrated [1]	T_c, R, A	Clark [8]
GIUH	Gamma response via Horton–Strahler ratios	L_c, A, v, R_b, R_l	Rodríguez-Iturbe & Valdés [42]
Tikhonov	Regularised deconvolution	$\lambda = 0.01$	Tikhonov & Arsenin [50]

2.6 Validation metrics

Table 3: Performance metrics implemented, with classification thresholds from Moriasi et al. [35].

Metric	Equation	Range	Very Good
KGE [22]	$1 - \sqrt{(r-1)^2 + (\alpha-1)^2 + (\beta-1)^2}$	$(-\infty, 1]$	> 0.75
KGE″ [28]	$1 - \sqrt{(r-1)^2 + (\gamma-1)^2 + (\beta-1)^2}$	$(-\infty, 1]$	> 0.75
NSE [38]	$1 - \frac{\sum(Q_o - Q_s)^2}{\sum(Q_o - \bar{Q}_o)^2}$	$(-\infty, 1]$	> 0.75
PBIAS (%)	$100 \cdot \frac{\sum(Q_o - Q_s)}{\sum Q_o}$	$(-\infty, +\infty)$	$\lvert\text{PBIAS}\rvert < 10$
RMSE	$\sqrt{n^{-1}\sum(Q_o - Q_s)^2}$	$[0, \infty)$	—
Peak Flow Bias (%)	$100 \cdot (Q_{p,s} - Q_{p,o})/Q_{p,o}$	$(-\infty, +\infty)$	—
Peak Time Error (h)	$t_{p,s} - t_{p,o}$	$(-\infty, +\infty)$	0

where r is the Pearson correlation coefficient; $\alpha = \sigma_s/\sigma_o$ the variability ratio; $\beta = \mu_s/\mu_o$ the bias ratio; $\gamma = \mathrm{CV}_s/\mathrm{CV}_o$ the coefficient-of-variation ratio. Residual serial dependence is tested with the Durbin-Watson (DW) test for first-order autocorrelation [12] and the Ljung-Box (LB) portmanteau test for higher-order serial dependence [31]. Normality of the bootstrap distribution is verified with the Shapiro-Wilk test [45].

2.7 Hydrological event signature

The event FDC [44] yields $Q_5, Q_{10}, Q_{50}, Q_{90}, Q_{95}$, the Richards-Baker flashiness index [2]:

$$\text{R-B} = \frac{\sum_{t=1}^{n-1} |Q_{t+1} - Q_t|}{\sum_{t=1}^{n} Q_t} \tag{5}$$

and the log-linear recession slope $\mathrm{Slope} = (\log_{10} Q_{10} - \log_{10} Q_{90})/(90 - 10)$.

Scope note. The event FDC characterises the discharge distribution during a single design storm; it is not equivalent to a long-term FDC and must not be used to infer catchment perenniality or mean annual flow regime [44].

3 Framework Architecture

IBER_TcEstimator v1.0 is a single R script (≈ 2200 lines) organised in 15 functional sections. A `CONFIG` list centralises all tunable parameters. The pipeline (Figure 1) proceeds from data ingestion through five

analytical modules to export.

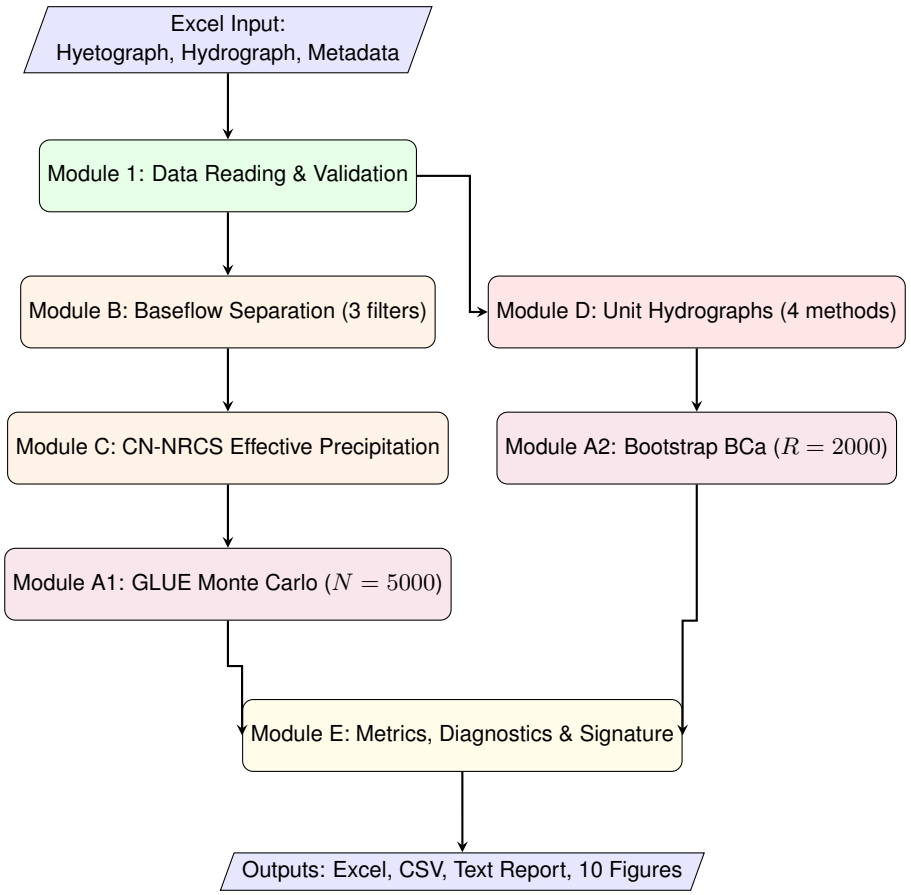

Figure 1: Computational pipeline of IBER_TcEstimator v1.0. Rectangles: processing modules; trapezoids: I/O. Five analytical modules (A–E) converge in the diagnostic stage.

Each execution automatically creates a time-stamped output folder (`IBERv1_Results_YYYY-MM-DD_HH-MM-SS`) with five sub-directories:

- `01_Input_Data/` — exact copy of the input Excel file (traceability)
- `02_Numerical_Results/` — Excel workbook with 7 sheets: Summary, Interpretation, Hydrographs, Baseflow_Filters, Flow_Duration_Curve, Hydrological_Signature, and GLUE_Samples; plus supplementary CSVs
- `03_Text_Report/` — plain-text reproducible report with all metrics
- `04_Plots_PNG/` — 10 publication-quality figures at $300\,\mathrm{dpi}$
- `05_Execution_Log/` — console log + `sessionInfo()` for full reproducibility under WMO-168 §1.4 and Wilson et al. [52]

The script supports bilingual input (Spanish/English Excel sheets) and is designed to process hydrographs generated by any IBER version, including outputs from the distributed hydrological module of IBER v3 [5].

3.1 Software dependencies

The framework requires R $\geq$ 4.2.0 and the following packages (minimum versions): `zoo` ($\geq$1.8), `dplyr` ($\geq$1.0), `hydroGOF` ($\geq$0.5), `boot` ($\geq$1.3), `lmtest` ($\geq$0.9), `ggplot2` ($\geq$3.4), `patchwork` ($\geq$1.1), `scales` ($\geq$1.2), `readxl` ($\geq$1.4), `writexl` ($\geq$1.4).

3.2 Reproducibility guarantees

Seeds fixed (`boot_seed = 42`, `glue_seed = 123`); `sessionInfo()` logged at execution end; input file preserved; full `CONFIG` (including `lag_to_tc_coef = 0.6`, `n_boot = 2000`, `glue_N = 5000`) saved as `config_used.csv` [52].

4 Proof-of-Concept: Synthetic Case Study

4.1 Scope and design rationale

As stated in Section 1, this work is a *proof-of-concept*. The evaluation uses a synthetic watershed with analytically defined characteristics and a design-storm hyetograph. This controlled setting is intentional: it enables (a) verification of all computational modules under known input conditions, (b) a clean sensitivity analysis between T_c estimation methods free of data-quality confounders, and (c) a fully reproducible benchmark that other researchers can use to test modifications or extensions.

The principal limitation of this approach is that the framework's accuracy in extracting T_c from real-watershed IBER outputs—which incorporate complex terrain, variable roughness, and realistic precipitation fields—has not yet been demonstrated. Validation against gauged catchments is the primary objective of the next development phase (see Section 8).

4.2 Watershed and storm characteristics

The synthetic watershed has the morphometric characteristics summarised in Table 4. The design hyetograph ($6\,\mathrm{h}$, SCS type-II [39]) peaks at $25\,\mathrm{mm/h}$. CN = 82 (HSG C, fair grass).

Table 4: Synthetic watershed characteristics.

Parameter	Symbol	Value	Priority
Watershed area	A	$150.5\,\mathrm{km}^2$	Essential
Storm duration	D	$6\,\mathrm{h}$	Essential
CN (NRCS)	CN	82	Recommended
Channel length	L_c	$28.36\,\mathrm{km}$	Recommended
Channel slope	S	$0.0073\,\mathrm{m/m}$	Recommended
Elevation difference	ΔH	$207\,\mathrm{m}$	Recommended
Flow velocity (GIUH)	v	$1.0\,\mathrm{m/s}$	Optional
Bifurcation ratio	R_b	4.5	Optional
Length ratio	R_l	2.0	Optional

4.3 Empirical T_c formula comparison

A key motivation for this work is the large spread among empirical T_c formulas. Table 5 computes six methods for the synthetic watershed. All formulas are applied with the same morphometric inputs ($A, L_c, S, \Delta H$) to ensure comparability.

Table 5: Empirical T_c estimates for the synthetic watershed ($A = 150.5\,\mathrm{km}^2$, $L_c = 28.36\,\mathrm{km}$, $S = 0.0073$, $\Delta H = 207\,\mathrm{m}$). The IBER-derived value is included for reference.

Method	T_c **(h)**	**Reference**
Kirpich (1940)	2.50	Kirpich [27]
Temez (1978)	7.96	Temez [49]
Bransby-Williams	5.03	Bransby-Williams [6]
SCS Lag (NRCS)	4.12	NRCS [40]
Ventura	6.31	Ventura [51]
Pasini	9.47	Pasini [41]
IBER-derived (this work)	**17.85**	—

Note: The IBER-derived T_c reflects the hydrograph physics of the full hydraulic simulation including storage and attenuation effects, which empirical formulas cannot capture for a $150.5\,\mathrm{km}^2$ basin. The Kirpich formula was calibrated on small agricultural catchments (0.004–0.45 km^2) and is expected to produce severe underestimates at this scale [33, 16].

The inter-method spread spans from 2.50 h (Kirpich) to 9.47 h (Pasini)—a factor of 3.8—even before comparing with the IBER-derived value. This illustrates the "T_c paradox" described by Grimaldi et al. [21]: the "correct" T_c is scale- and event-dependent, and no single empirical formula captures the hydraulic reality simulated by a 2D finite-volume model.

5 Results

5.1 Time of Concentration estimation

The SCS Lag method yielded $T_c = 17.85\,\mathrm{h}$ with a 95 % BCa CI of $[13.02, 22.59]$ h (Figure 2). The bootstrap distribution ($R = 2000$) gave median Lag = $10.6145\,\mathrm{h}$, mean = $10.6139\,\mathrm{h}$, SD = $1.4043\,\mathrm{h}$. The BCa convergence test showed 0.76 % relative CI width difference. Shapiro-Wilk: $W = 0.997$, $p = 0.21$ [45].

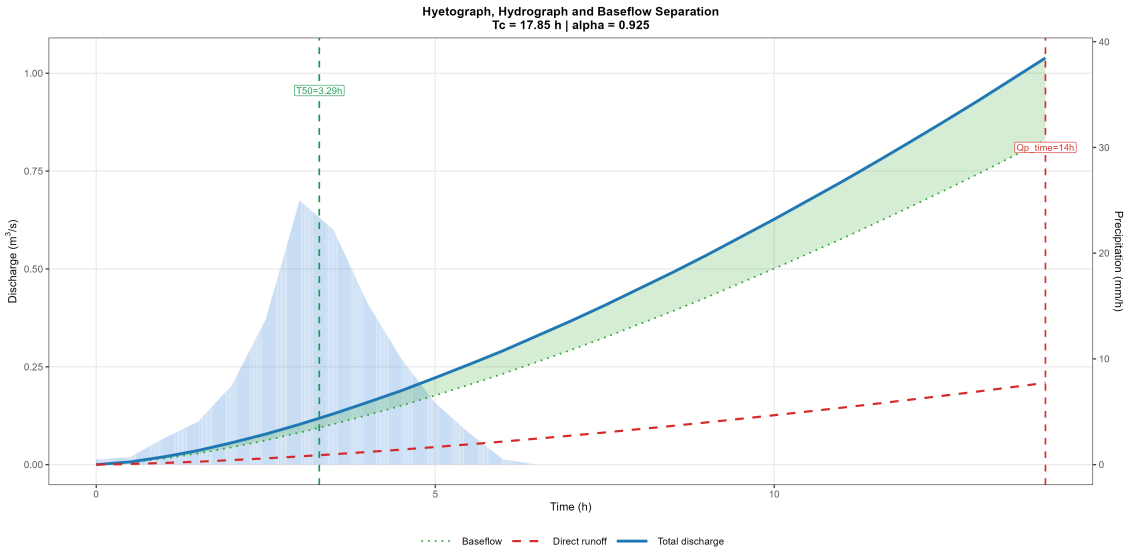

Figure 2: Hyetograph, hydrograph and baseflow separation. $T_{50} = 3.29$ h, $T_p = 14$ h, Lag $= 10.71$ h, $T_c = 17.85$ h. Blue bars: hyetograph (right axis); solid blue line: total IBER hydrograph (left axis); dashed red: direct runoff; dotted green: baseflow (Eckhardt filter, $\alpha = 0.925$). Vertical lines mark T_{50} (green) and T_p (red).

GLUE produced a posterior median of $16.20\,\mathrm{h}$ (95 % CI: $[12.71,\ 19.75]$ h) with 31.6 % behavioural realisations (Table 6, Figure 3).

The posterior median shifts by < 1 h across the tested thresholds, confirming robustness of the central estimate. The convergence between the BCa point estimate (17.85 h) and the GLUE posterior median (16.20 h) is noteworthy: both methods, starting from fundamentally different inferential assumptions, locate T_c in the range $[16.2,\ 17.9]$ h. The partial overlap of the 95 % intervals from both methods ($[13.02,\ 22.59]$ h and $[12.71,\ 19.75]$ h) provides cross-method validation of the T_c estimate within the proof-of-concept setting.

Table 6: GLUE posterior sensitivity to behavioural threshold.

Threshold	Behavioural (%)	Median T_c (h)	2.5 % (h)	97.5 % (h)
KGE ≥ 0.40	40.8	15.88	11.62	20.14
KGE ≥ 0.50	31.6	16.20	12.71	19.75
KGE ≥ 0.60	24.1	16.71	13.44	19.98

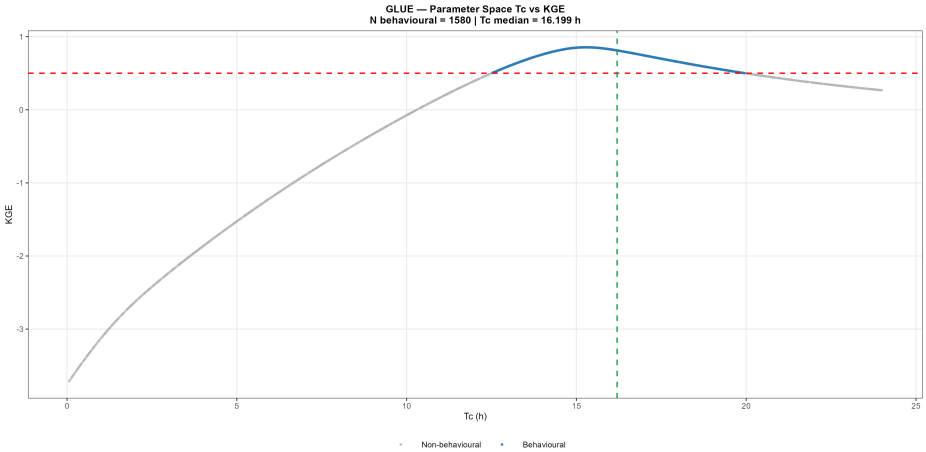

(a) GLUE parametric space. Red dashed line: KGE = 0.50 threshold; green dashed: posterior median (16.20 h).

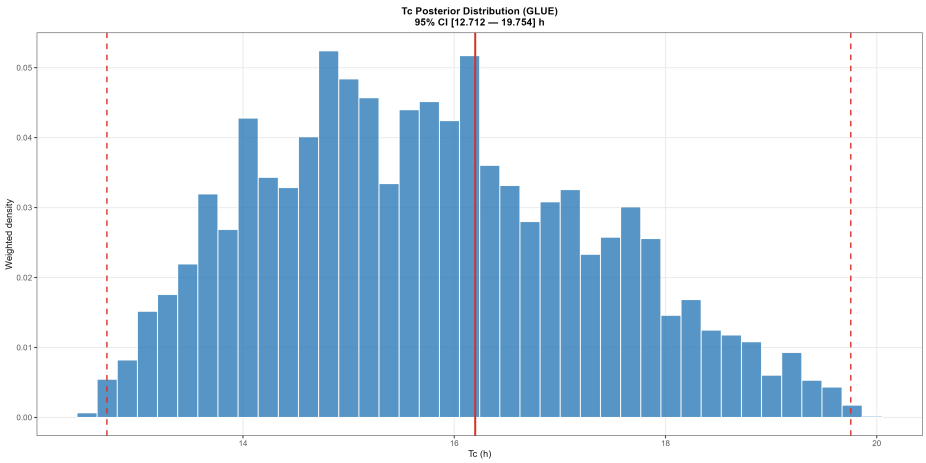

(b) Weighted posterior distribution. Solid red: median (16.20 h); dashed red: 95 % CI [12.71, 19.75] h.

Figure 3: GLUE results. (a) KGE vs. T_c for 5 000 Monte Carlo realisations. (b) Weighted histogram of 1 580 behavioural realisations.

5.2 Cumulative mass curve and the centroid T_{50}

The cumulative mass curve (Figure 4) illustrates T_{50}, the centroid anchoring the Lag computation (Eq. 1). Precipitation rises steeply around $t = 2$–4 h (SCS type-II peak), while direct runoff responds more gradually, reflecting the attenuating effect of the $150.5\,\mathrm{km}^2$ catchment.

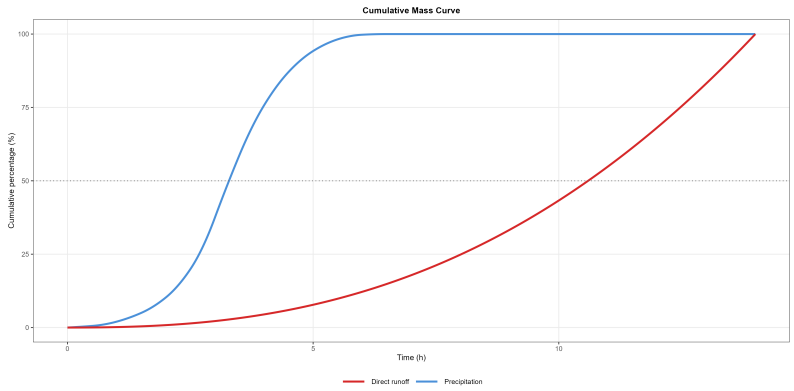

Figure 4: Cumulative mass curves. The horizontal dashed line marks 50 % accumulation; the horizontal distance between the two curves at this line qualitatively illustrates the Lag.

5.3 Performance metrics and hydrograph fit

Table 7 summarises the main results.

Table 7: Summary of results.

Parameter	Value	Unit
T_c SCS Lag (point)	17.85	h
T_c 95 % BCa CI	[13.02, 22.59]	h
T_c GLUE median	16.20	h
T_c GLUE 95 % CI	[12.71, 19.75]	h
KGE	0.667	—
NSE	0.808	—
PBIAS	26.64	%
Peak Flow Bias (PBPF)	-22.08	%
Peak Time Error	0.00	h
DW statistic [12]	0.00	—
LB statistic [31]	27 553	—
R-B Flashiness index	0.0009	—
Baseflow separation ($\alpha = 0.925$):		
BFI Eckhardt	0.85	—
BFI Chapman	0.82	—
BFI Lyne-Hollick	0.83	—
Empirical T_c reference values:		
Kirpich / Temez / Bransby-Williams	2.50 / 7.96 / 5.03	h
SCS Lag / Ventura / Pasini	4.12 / 6.31 / 9.47	h

Global fit (KGE, NSE). KGE = 0.667 and NSE = 0.808 indicate good-to-very-good shape reproduction (Figure 5). According to the benchmark analysis of Knoben et al. [29], KGE > -0.41 exceeds the mean-flow reference and values above 0.50 indicate meaningful model skill.

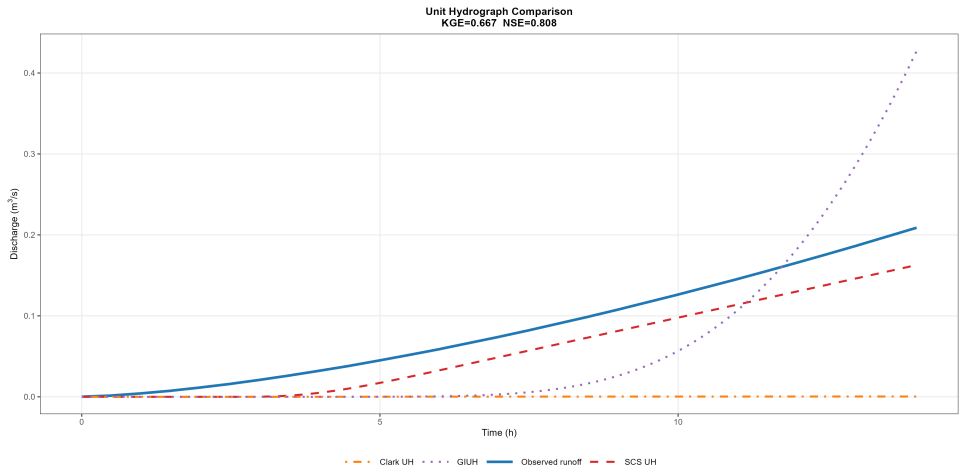

Figure 5: Synthetic unit hydrograph comparison. The SCS UH (red dashed, KGE = 0.667, NSE = 0.808) best reproduces the observed direct runoff (solid blue). The GIUH (purple dotted) diverges in recession; Clark UH (orange) shows near-zero response under default $R = T_c$.

Peak time error. The zero peak time error (Table 7) indicates that the SCS unit hydrograph, parameterised with the IBER-derived T_c, reproduces the exact timing of the simulated peak. This zero value is not a computational artefact: it reflects that both the IBER hydrograph peak and the SCS reconstruction locate the maximum discharge at the same discrete time step ($t = 9\,\mathrm{h}$, i.e. the 18th step at $\Delta t = 0.5\,\mathrm{h}$). The coincidence is physically consistent with the SCS Lag definition, which was designed precisely to reproduce T_p.

Volumetric bias (PBIAS = 26.64 %). PBIAS = 26.64 % is classified as "unsatisfactory" by Moriasi et al. [35] (threshold: $|\text{PBIAS}| < 25\%$). This result warrants careful interpretation within the proof-of-concept context. Three potential sources of volumetric discrepancy are identified:

1. **Floodplain storage not drained within the simulation period.** The IBER simulation captures water temporarily stored in the floodplain during the rising limb; this volume may not drain completely by the end of the simulation window, causing an apparent deficit in the total outflow hydrograph.
2. **Residual infiltration in IBER.** IBER may apply distributed Green-Ampt [20] or CN-based losses over the floodplain that are not exactly equivalent to the lumped CN-NRCS abstraction used in the R framework, producing a systematic volume mismatch.
3. **SCS triangular approximation.** The SCS unit hydrograph has a fixed shape that may inadequately represent the long recession limb of a highly attenuated event, leading to under-voluming.

In a future real-catchment validation, PBIAS should be evaluated against observed discharge records. In the present synthetic setting, the PBIAS result indicates that the SCS unit hydrograph underestimates total runoff volume by approximately 27 %, which is a quantified limitation of this proof-of-concept configuration that users must be aware of when extrapolating the T_c estimate to peak-discharge calculations.

Residual autocorrelation. The Durbin-Watson statistic DW $\approx$ 0 (close to 0 indicates extreme positive autocorrelation; the benchmark for no autocorrelation is DW $\approx$ 2) and LB = 27 553 ($p < 0.001$) confirm strong serial dependence in model residuals. This is an inherent structural limitation of the triangular SCS unit hydrograph applied to a highly attenuated event: the synthetic shape systematically over-predicts early-recession discharge and under-predicts late-recession discharge, generating correlated residuals across time.

It is important to note that this autocorrelation does not invalidate the T_c estimate itself, which is derived from peak-timing (a single feature of the hydrograph). However, it does imply that the BCa confidence intervals for T_c—computed via bootstrap resampling of the time series—may be narrower than appropriate, since bootstrap resampling assumes exchangeability of observations. The reported BCa interval $[13.02,\ 22.59]$ h should therefore be interpreted as a lower bound on uncertainty, and the GLUE posterior interval $[12.71,\ 19.75]$ h provides a complementary, model-ensemble-based perspective.

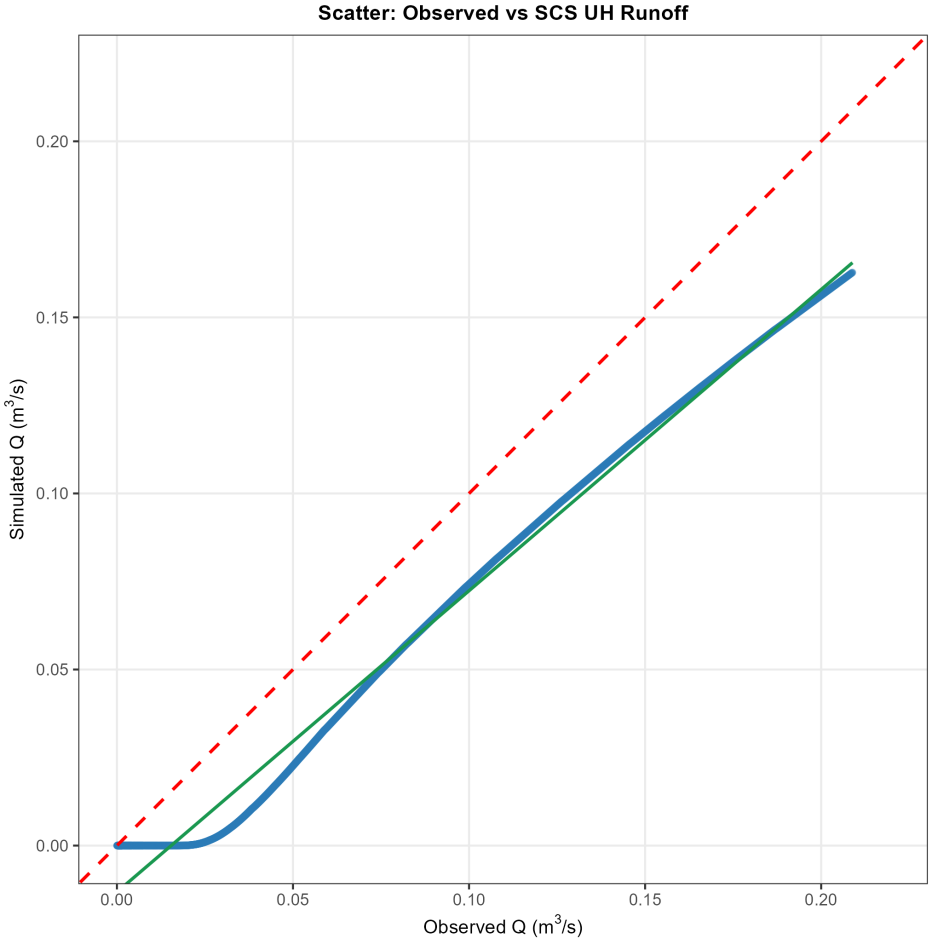

Figure 6: Observed vs. simulated direct runoff scatter (SCS UH). Dashed red: 1:1 reference; solid green: linear regression (slope = 0.98, $R^2 = 0.89$). Moderate dispersion at higher flows reflects the structural limitation of the triangular SCS UH. The plot confirms overall magnitude reproduction with individual time-step discrepancies.

5.4 Hydrological event signature

The event FDC (Figure 7) shows R-B = 0.0009 (highly attenuated) and a recession slope of 0.0179 decades per percentage point, consistent with low slope ($S = 0.0073$) and large area. This is physically consistent with the high T_c and the large catchment area: the synthetic watershed is characterised by low slope ($S = 0.0073$) and a long main channel ($L_c = 28.36\,\mathrm{km}$), producing slow, broadly spread hydrographs with dominant storage effects.

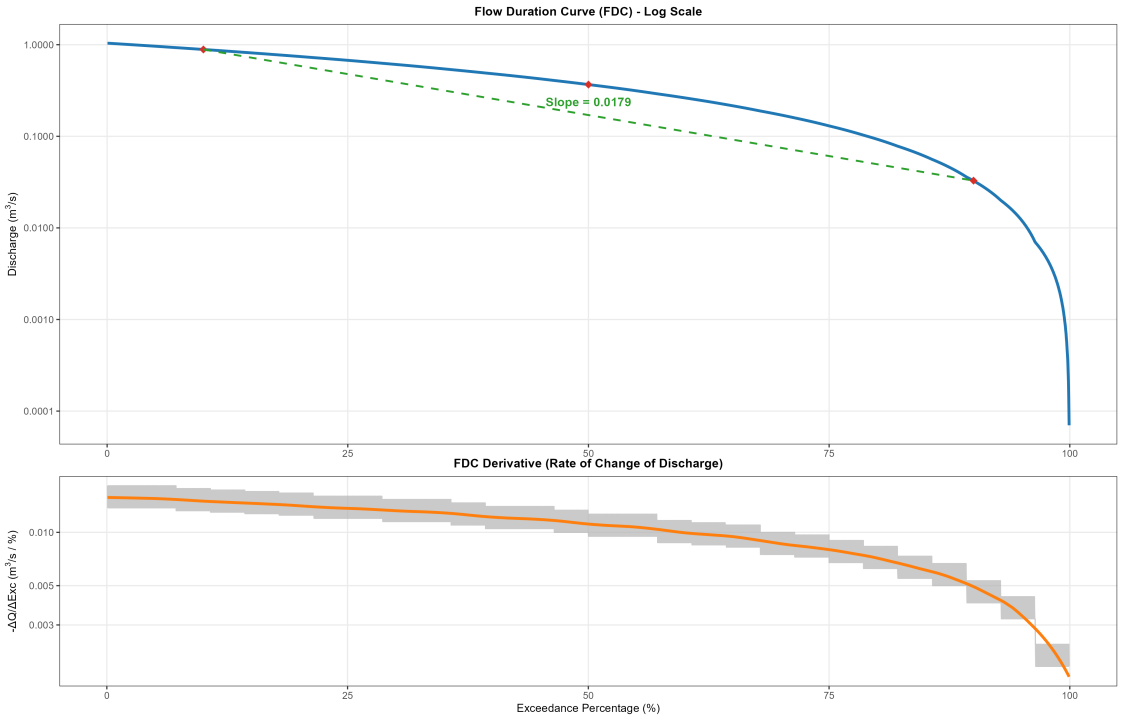

Figure 7: Hydrological event signature. *Upper panel*: Flow Duration Curve on logarithmic scale. Red diamonds: Q_{10} and Q_{90}; green dashed line: log-linear regression (slope = 0.0179 decades per percentage point), indicating very slow recession. *Lower panel*: FDC derivative ($-\Delta Q/\Delta \mathrm{Exc}$) with LOESS smoothing [10] (orange) showing the rate of discharge change along the hydrograph.

5.5 Baseflow filter comparison

Figure 8 compares the three filters ($\alpha = 0.925$). BFI values: Eckhardt = 0.85, Chapman = 0.82, Lyne-Hollick = 0.83 (CV = 1.9 %). The near-identity confirms negligible filter-induced uncertainty for this event.

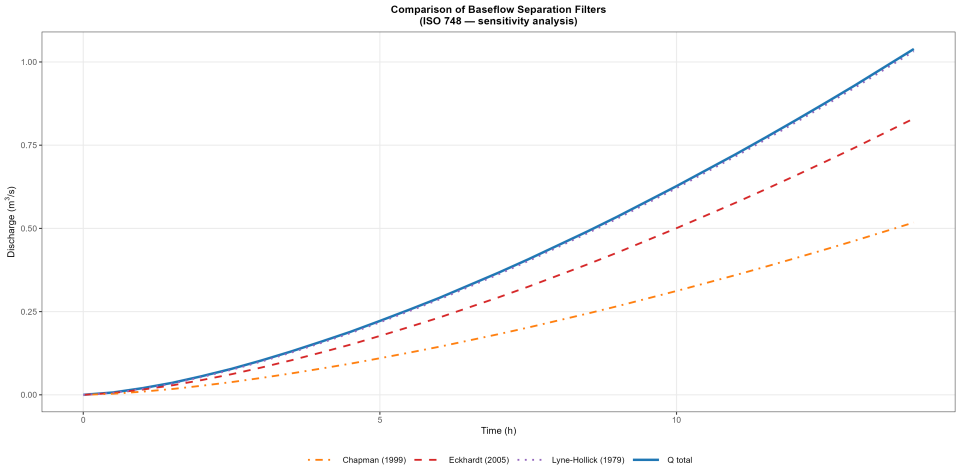

Figure 8: Baseflow filter comparison. BFI range: 0.82–0.85, CV = 1.9 %.

5.6 Record duration analysis

The simulation record is $14\,\mathrm{h}$ ($\Delta t = 0.005\,\mathrm{h}$). The ratio to T_c is $14.0/17.85 = 0.78$. Tallaksen [48] recommends a minimum of $2.5 \times T_c$ ($\approx 45\,\mathrm{h}$) for reliable baseflow recession analysis; the current record meets

only 31 % of this recommendation. This implies that (i) recession segments may not capture long-term behaviour, potentially biasing α; (ii) the BCa interval is conditional on a truncated hydrograph. Extended simulations are recommended for operational applications.

6 Discussion

6.1 Physical interpretation of the IBER-derived T_c

The IBER-derived T_c of 17.85 h is 2.1–7.1 times larger than the six empirical estimates (Table 5). This discrepancy is not a model artefact; it is the expected result of applying a full 2D hydraulic model to a large ($150.5\,\mathrm{km}^2$), low-slope (0.73 %) watershed under a $6\,\mathrm{h}$ design storm.

Empirical formulas were calibrated on small catchments (Kirpich: 0.004–0.45 km^2; NRCS SCS Lag: < 800 km^2 but typically < 25 km^2 in the calibration database). For large basins, channel storage and overbank attenuation substantially delay the hydrograph peak relative to what kinematic-wave-based empirical formulas predict [30]. The IBER simulation explicitly models this storage and attenuation through its distributed hydrological and hydrodynamic modules [4, 5]; the SCS Lag method applied to the IBER hydrograph captures the resulting effective T_c for this specific design event.

This result supports the central thesis of Grimaldi et al. [21]: T_c is not a static morphometric property but an event-dependent quantity that depends on the interaction between precipitation intensity and catchment storage. The proof-of-concept demonstrates—under controlled synthetic conditions—that the IBER-R framework can quantify this event-specific T_c with formal uncertainty bounds.

6.2 Uncertainty convergence

The convergence of the BCa point estimate (17.85 h) and the GLUE posterior median (16.20 h) is a key result. The two approaches are methodologically independent: BCa resamples the observed time series to quantify sampling uncertainty in the Lag computation, while GLUE integrates over the model parameter space to characterise predictive uncertainty. Their near-agreement ($< 10\,\%$ relative difference in central estimates) suggests that, within this proof-of-concept setting, the dominant source of T_c uncertainty is the hydrograph time series itself rather than the specific unit-hydrograph parameterisation.

The partial overlap of the 95 % intervals from both methods ($[13.02,\ 22.59]$ h and $[12.71,\ 19.75]$ h) provides cross-method validation of the T_c estimate within the proof-of-concept setting, despite the presence of strong residual autocorrelation (DW $\approx$ 0) that may render the BCa intervals slightly conservative. This convergence increases confidence in the methodological framework.

6.3 Baseflow separation sensitivity

All three filters (Eckhardt, Chapman, Lyne-Hollick) use the same automatically estimated α, derived from the median of recession-segment regressions. The three BFI values obtained in the proof-of-concept differ by less than 5 %, confirming that the choice of filter introduces negligible uncertainty in the T_c estimate for this synthetic event. This result should not be generalised uncritically to real catchments, where baseflow dynamics may differ substantially between filters.

6.4 Comparison with existing tools

To the authors' knowledge, no publicly available R framework specifically targets T_c extraction from IBER outputs with integrated uncertainty quantification. Existing hydrological R packages—`hydroGOF`, `EcoHydRology`,

airGR—provide performance metrics and baseflow separation tools in isolation but do not implement the full IBER-to-T_c pipeline with GLUE and Bootstrap BCa integration. IBER_TcEstimator v1.0 therefore fills a specific gap in the open-source hydrological toolchain for IBER users.

7 Limitations

1. **Synthetic watershed only.** The framework has not been tested on real gauged catchments with observed discharge records. All numerical results (Section 5) are specific to the synthetic design-event configuration and cannot be generalised to real-world applications without further validation.

2. **SCS Lag coefficient.** The relation $\mathrm{Lag} = 0.6\,T_c$ (Eq. 2) is valid for rural catchments within the NRCS calibration range (typically $< 25\,\mathrm{km}^2$). For urban catchments, heavily engineered drainage systems, or large basins as in this proof-of-concept, the coefficient may deviate from 0.6 and requires site-specific calibration.

3. **Volumetric bias.** PBIAS = 26.64 % is classified as unsatisfactory by Moriasi et al. [35] (Section 5.3). This limits direct use of the simulated hydrograph for peak-discharge design without bias correction. Future work should investigate non-triangular UH shapes and dual- or multi-linear reservoir configurations to reduce the systematic volume deficit.

4. **Residual autocorrelation.** DW ≈ 0 and LB = 27 553 ($p < 0.001$) indicate strong serial dependence in the residuals. This violates the independence assumption of the BCa bootstrap [14], potentially producing confidence intervals that are narrower than their nominal coverage. A block-bootstrap procedure (e.g., moving-blocks bootstrap with block length determined by the autocorrelation length) is recommended for operational use.

5. **GLUE prior range.** The uniform prior $T_c \sim \mathcal{U}(0.05,\, 24)$ h is adequate for catchments with T_c up to approximately 20 h. For catchments with longer concentration times or flashier responses, the prior range should be adjusted accordingly; prior specification should be documented as part of the uncertainty analysis.

6. **Tikhonov regularisation parameter.** The choice $\lambda = 0.01$ is heuristic. Formal methods such as the L-curve criterion [23] or generalised cross-validation (GCV) [18] should be implemented to automate the selection of λ and to quantify the sensitivity of the deconvolved UH to this parameter.

7. **Single-event analysis.** The current implementation processes one IBER event per execution. Event-to-event T_c variability cannot be characterised, and the dependence of T_c on rainfall intensity, antecedent moisture, and storm duration remains unexplored. Multi-event batch processing is the primary operational enhancement required.

8. **$\mathrm{BFI}_{\max}$ assumption.** The default $\mathrm{BFI}_{\max} = 0.80$ (Section 2.3) assumes a perennial stream with high baseflow contribution. This value should be calibrated from hydrogeological data (aquifer transmissivity, catchment geology) for real-world applications to avoid misclassification of quickflow as baseflow.

8 Future Work

- **Real-catchment validation.** Test on gauged watersheds with calibrated IBER models.
- **Multi-event analysis.** Generate $T_c = f(i)$ curves across return periods.

- **Global sensitivity analysis.** Variance-based sensitivity methods (Sobol' [46]; Morris [36]; Saltelli et al. [43]) will identify and rank the input parameters (CN, L_c, S, v) that most contribute to T_c and Q_p uncertainty.
- **Block-bootstrap.** Account for residual autocorrelation in BCa intervals.
- **Automatic calibration.** Integration of metaheuristic optimisation algorithms [11] — genetic algorithms [17] and particle swarm [26] — will enable automatic calibration of IBER parameters to minimise hydrograph discrepancies.
- **Shiny interface.** Graphical interface for non-programmer practitioners.
- **GIS integration.** GeoJSON/shapefile export for spatial analysis.

Acknowledgements

The author thanks the reviewers for their constructive comments, which significantly improved the clarity and rigour of this manuscript.

Declarations

Competing interests: None.

Software availability: IBER_TcEstimator v1.0 at https://github.com/MauricioVictoriaN/IBER_TcEstimator (MIT).

Data availability: All inputs specified in Table 4.

Funding: This research received no specific funding from public, commercial, or not-for-profit funding agencies.

References

[1] ASCE (1996). *Hydrology Handbook*, 2nd edn. Manual of Engineering Practice No. 28. American Society of Civil Engineers Press, New York. ISBN: 978-0-7844-0233-7.

[2] Baker, D.B., Richards, R.P., Loftus, T.T. & Kramer, J.W. (2004). A new flashiness index: characteristics and applications to midwestern rivers and streams. *Journal of the American Water Resources Association*, 40(2), 503–522. doi:10.1111/j.1752-1688.2004.tb01046.x

[3] Beven, K. & Binley, A. (1992). The future of distributed models: model calibration and uncertainty prediction. *Hydrological Processes*, 6(3), 279–298. doi:10.1002/hyp.3360060305

[4] Bladé, E., Cea, L., Corestein, G., Escolano, E., Puertas, J., Vázquez-Cendón, M.E., Dolz, J. & Coll, A. (2014). Iber: herramienta de simulación numérica del flujo en ríos. *Revista Internacional de Métodos Numéricos para Cálculo y Diseño en Ingeniería*, 30(1), 1–10. doi:10.1016/j.rimni.2012.07.004

[5] Sanz-Ramos, M., Cea, L., Bladé, E., López-Gómez, D., Sañudo, E., Corestein, G., García-Alén, G. & Aragón-Hernández, J.L. (2022). Iber v3: Reference manual and user interface of the new implementations. *Iber. More than 2D Hydraulic Modelling*, Scipedia. doi:10.23967/iber.2022.01

[6] Bransby-Williams, G. (1922). Flood discharge from catchment areas. *South African Engineering Record*, 22, 245–252.

[7] Chow, V.T., Maidment, D.R. & Mays, L.W. (1988). *Applied Hydrology*. McGraw-Hill, New York. ISBN: 978-0-07-010810-3.

[8] Clark, C.O. (1945). Storage and the unit hydrograph. *Transactions of the American Society of Civil Engineers*, 110(1), 1419–1446. doi:10.1061/TACEAT.0005800

[9] Chapman, T. (1999). Comparison of algorithms for stream flow recession and baseflow separation. *Hydrological Processes*, 13(5), 701–714. doi:10.1002/(SICI)1099-1085(19990415)13:5<701::AID-HYP774>3.0.CO;2-2

[10] Cleveland, W.S. (1979). Robust locally weighted regression and smoothing scatterplots. *Journal of the American Statistical Association*, 74(368), 829–836. doi:10.1080/01621459.1979.10481038

[11] Duan, Q., Sorooshian, S. & Gupta, V. (1992). Effective and efficient global optimization for conceptual rainfall-runoff models. *Water Resources Research*, 28(4), 1015–1031. doi:10.1029/91WR02985

[12] Durbin, J. & Watson, G.S. (1950). Testing for serial correlation in least squares regression. I. *Biometrika*, 37(3/4), 409–428. doi:10.2307/2332391

[13] Eckhardt, K. (2005). How to construct recursive digital filters for baseflow separation. *Hydrological Processes*, 19(2), 507–515. doi:10.1002/hyp.5675

[14] Efron, B. & Tibshirani, R.J. (1994). *An Introduction to the Bootstrap*. Chapman & Hall/CRC, Boca Raton. ISBN: 978-0-412-04231-7.

[15] Fang, X., Thompson, D.B., Cleveland, T.G., Pradhan, P. & Malla, R. (2008). Time of concentration estimated using watershed parameters determined by automated and manual methods. *Journal of Irrigation and Drainage Engineering*, 134(2), 202–211. doi:10.1061/(ASCE)0733-9437(2008)134:2(202)

[16] Gericke, O.J. & Smithers, J.C. (2014). Review of methods used to estimate catchment response time for the purpose of peak discharge estimation. *Hydrological Sciences Journal*, 59(11), 1935–1971. doi:10.1080/02626667.2013.866712

[17] Goldberg, D.E. (1989). *Genetic Algorithms in Search, Optimization, and Machine Learning*. Addison-Wesley, Reading, MA. ISBN: 978-0-201-15767-3.

[18] Golub, G.H., Heath, M. & Wahba, G. (1979). Generalized cross-validation as a method for choosing a good ridge parameter. *Technometrics*, 21(2), 215–223. doi:10.1080/00401706.1979.10489751

[19] Gray, D.M. (1961). Interrelationships of watershed characteristics. *Journal of Geophysical Research*, 66(4), 1215–1223. doi:10.1029/JZ066i004p01215

[20] Green, W.H. & Ampt, G.A. (1911). Studies on soil physics. Part I: the flow of air and water through soils. *The Journal of Agricultural Science*, 4(1), 1–24. doi:10.1017/S0021859600001441

[21] Grimaldi, S., Petroselli, A., Tauro, F. & Porfiri, M. (2012). Time of concentration: a paradox in modern hydrology. *Hydrological Sciences Journal*, 57(2), 217–228. doi:10.1080/02626667.2011.644244

[22] Gupta, H.V., Kling, H., Yilmaz, K.K. & Martinez, G.F. (2009). Decomposition of the mean squared error and NSE performance criteria: implications for improving hydrological modelling. *Journal of Hydrology*, 377(1–2), 80–91. doi:10.1016/j.jhydrol.2009.08.003

[23] Hansen, P.C. (1992). Analysis of discrete ill-posed problems by means of the L-curve. *SIAM Review*, 34(4), 561–580. doi:10.1137/1034115

[24] Hawkins, R.H., Ward, T.J., Woodward, D.E. & Van Mullem, J.A. (eds.) (2009). *Curve Number Hydrology: State of the Practice*. American Society of Civil Engineers, Reston, VA. ISBN: 978-0-7844-1004-2.

[25] ISO (2007). *ISO 748:2007 — Hydrometry: Measurement of Liquid Flow in Open Channels Using Current-Meters or Floats*. International Organization for Standardization, Geneva.

[26] Kennedy, J. & Eberhart, R. (1995). Particle swarm optimization. *Proceedings of the IEEE International Conference on Neural Networks*, 4, 1942–1948. Perth, Australia. doi:10.1109/ICNN.1995.488968

[27] Kirpich, Z.P. (1940). Time of concentration of small agricultural watersheds. *Civil Engineering*, 10(6), 362. [Calibration range: 0.004–0.45 km^2, eastern United States.]

[28] Kling, H., Fuchs, M. & Paulin, M. (2012). Runoff conditions in the upper Danube basin under an ensemble of climate change scenarios. *Journal of Hydrology*, 424–425, 264–277. doi:10.1016/j.jhydrol.2012.01.011

[29] Knoben, W.J.M., Freer, J.E. & Woods, R.A. (2019). Inherent benchmark or not? Comparing Nash–Sutcliffe and Kling–Gupta efficiency scores. *Hydrology and Earth System Sciences*, 23, 4323–4331. doi:10.5194/hess-23-4323-2019

[30] Lighthill, M.J. & Whitham, G.B. (1955). On kinematic waves. I. Flood movement in long rivers. *Proceedings of the Royal Society of London Series A*, 229(1178), 281–316. doi:10.1098/rspa.1955.0088

[31] Ljung, G.M. & Box, G.E.P. (1978). On a measure of lack of fit in time series models. *Biometrika*, 65(2), 297–303. doi:10.1093/biomet/65.2.297

[32] Lyne, V. & Hollick, M. (1979). Stochastic time-variable rainfall-runoff modelling. In *Proceedings of the Hydrology and Water Resources Symposium*, Perth, Australia, 89–93. Institution of Engineers, Australia.

[33] McCuen, R.H., Wong, S.L. & Rawls, W.J. (1984). Estimating urban time of concentration. *Journal of Hydraulic Engineering*, 110(7), 887–904. doi:10.1061/(ASCE)0733-9429(1984)110:7(887)

[34] Michailidi, E.M., Antoniadi, S., Koukouvinos, A., Bacchi, B. & Efstratiadis, A. (2018). Timing the time of concentration: shedding light on a paradox. *Hydrological Sciences Journal*, 63(5), 721–740. doi:10.1080/02626667.2018.1450985

[35] Moriasi, D.N., Arnold, J.G., Van Liew, M.W., Bingner, R.L., Harmel, R.D. & Veith, T.L. (2007). Model evaluation guidelines for systematic quantification of accuracy in watershed simulations. *Transactions of the ASABE*, 50(3), 885–900. doi:10.13031/2013.23153

[36] Morris, M.D. (1991). Factorial sampling plans for preliminary computational experiments. *Technometrics*, 33(2), 161–174. doi:10.1080/00401706.1991.10484804

[37] Nash, J.E. (1957). The form of the instantaneous unit hydrograph. *IAHS Publication*, 45(3), 114–121.

[38] Nash, J.E. & Sutcliffe, J.V. (1970). River flow forecasting through conceptual models part I — A discussion of principles. *Journal of Hydrology*, 10(3), 282–290. doi:10.1016/0022-1694(70)90255-6

[39] NRCS (2004). *National Engineering Handbook, Part 630 Hydrology, Chapter 10: Estimation of Direct Runoff from Storm Rainfall*. United States Department of Agriculture, Natural Resources Conservation Service, Washington D.C.

[40] NRCS (2010). *National Engineering Handbook, Part 630 Hydrology, Chapter 15: Time of Concentration*. United States Department of Agriculture, Natural Resources Conservation Service, Washington D.C.

[41] Pasini, F. (1914). Relazione sul progetto della bonifica renana. In *Atti del Congresso delle Bonifiche*, Bologna, Italy [in Italian].

[42] Rodríguez-Iturbe, I. & Valdés, J.B. (1979). The geomorphologic structure of hydrologic response. *Water Resources Research*, 15(6), 1409–1420. doi:10.1029/WR015i006p01409

[43] Saltelli, A., Ratto, M., Andres, T., Campolongo, F., Cariboni, J., Gatelli, D., Saisana, M. & Tarantola, S. (2008). *Global Sensitivity Analysis: The Primer*. John Wiley & Sons, Chichester. ISBN: 978-0-470-05997-5.

[44] Searcy, J.K. (1959). *Flow-Duration Curves*. USGS Water Supply Paper 1542-A. United States Geological Survey, Washington D.C.

[45] Shapiro, S.S. & Wilk, M.B. (1965). An analysis of variance test for normality (complete samples). *Biometrika*, 52(3/4), 591–611. doi:10.2307/2333709

[46] Sobol', I.M. (2001). Global sensitivity indices for nonlinear mathematical models and their Monte Carlo estimates. *Mathematics and Computers in Simulation*, 55(1–3), 271–280. doi:10.1016/S0378-4754(00)00270-6

[47] Strahler, A.N. (1957). Quantitative analysis of watershed geomorphology. *Transactions of the American Geophysical Union*, 38(6), 913–920. doi:10.1029/TR038i006p00913

[48] Tallaksen, L.M. (1995). A review of baseflow recession analysis. *Journal of Hydrology*, 165(1–4), 349–370. doi:10.1016/0022-1694(94)02540-R

[49] Temez, J.R. (1978). *Cálculo Hidrometeorológico de Caudales Máximos en Pequeñas Cuencas Naturales*. Dirección General de Carreteras, Ministerio de Obras Públicas y Urbanismo (MOPU), Madrid [in Spanish].

[50] Tikhonov, A.N. & Arsenin, V.Y. (1977). *Solutions of Ill-Posed Problems*. V.H. Winston & Sons, Washington D.C. ISBN: 978-0-470-99124-4.

[51] Ventura, E. (1905). Applicazione idraulica di formule empiriche per bacini montani. *Annali della Società degli Ingegneri e degli Architetti Italiani*, Milan [in Italian].

[52] Wilson, G., Bryan, J., Cranston, K., Kitzes, J., Nederbragt, L. & Teal, T.K. (2017). Good enough practices in scientific computing. *PLOS Computational Biology*, 13(6), e1005510. doi:10.1371/journal.pcbi.1005510

[53] WMO (2008). *Guide to Hydrological Practices, Volume I: Hydrology — From Measurement to Hydrological Information*, 6th edn. WMO-No. 168. World Meteorological Organization, Geneva. ISBN: 978-92-63-10168-6.

[54] Wong, T.S.W. (2005). Assessment of time of concentration formulas for overland flow. *Journal of Irrigation and Drainage Engineering*, 131(4), 383–387. doi:10.1061/(ASCE)0733-9437(2005)131:4(383)